

# Mesenchymal stem cell-derived extracellular vesicles may promote breast cancer cell dormancy

Journal of Tissue Engineering  
Volume 9: 1–7  
© The Author(s) 2018  
Article reuse guidelines:  
[sagepub.com/journals-permissions](http://sagepub.com/journals-permissions)  
DOI: 10.1177/2041731418810093  
[journals.sagepub.com/home/tej](http://journals.sagepub.com/home/tej)



Jake Casson<sup>1</sup> , Owen G Davies<sup>2</sup>, Carol-Anne Smith<sup>1</sup>,  
Matthew J Dalby<sup>1</sup> and Catherine C Berry<sup>1</sup>

## Abstract

Disseminated breast cancer cells have the capacity to metastasise to the bone marrow and reside in a dormant state within the mesenchymal stem cell niche. Research has focussed on paracrine signalling factors, such as soluble proteins, within the microenvironment. However, it is now clear extracellular vesicles secreted by resident mesenchymal stem cells into this microenvironment also play a key role in the initiation of dormancy. Dormancy encourages reduced cell proliferation and migration, while upregulating cell adhesion, thus retaining the cancer cells within the bone marrow microenvironment. Here, MCF7 breast cancer cells were treated with mesenchymal stem cell-derived extracellular vesicles, resulting in reduced migration in two-dimensional and three-dimensional culture, with reduced cell proliferation and enhanced adhesion, collectively supporting cancer cell dormancy.

## Keywords

Breast cancer, mesenchymal stem cell, extracellular vesicle, dormancy, three dimensional

Date received: 8 July 2018; accepted: 10 October 2018

## Introduction

Breast cancer is the most prevalent form of malignancy in women.<sup>1</sup> Dissemination of breast cancer cells (BCCs) to distant sites is believed to be an early event, often occurring before detection of the primary tumour.<sup>2</sup> More than two-thirds of breast cancers that spread to other parts of the body spread to the bone marrow.<sup>3</sup> It is now well established that breast cancer recurrence is due to prolonged dormancy within the bone marrow.<sup>4</sup> This phenomenon is responsible for much of the cancer-associated mortality as metastatic recurrence can occur many years after primary tumour treatment, leading to an uncertainty in the prognosis for patients.<sup>5</sup>

Prior to metastasis, BCCs undergo epithelial–mesenchymal transition (EMT), whereby they lose epithelial traits such as cell adhesion and gain mesenchymal characteristics, becoming migratory.<sup>6,7</sup> Upon reaching distant secondary sites, such as the bone marrow, a reverse process termed mesenchymal–epithelial transition (MET) then occurs, allowing the BCCs to colonise their secondary microenvironment.<sup>8</sup>

The invading BCCs take advantage of the immune tolerant features and chemotactic properties of resident mesenchymal stem cells (MSCs) and their niche to both promote and support BCC dormancy.<sup>9,10</sup> In the early stages of metastatic spread, disseminated BCCs undergo an extended period of cycling quiescence in which they are maintained in G<sub>0</sub>/G<sub>1</sub> phase of the cell cycle.<sup>11</sup> However, there is a current lack of knowledge of the mechanistic events that allow BCCs to adopt a dormant phenotype in the marrow.<sup>12</sup> MSCs are thought to interact with invading BCCs during the early stage of entry into the marrow; thus, further study of how these two

<sup>1</sup>Centre for Cell Engineering, Institute of Molecular, Cell and Systems Biology (IMCSB), The University of Glasgow, Glasgow, UK

<sup>2</sup>School of Sport, Exercise and Health Sciences, Loughborough University, Loughborough, UK

### Corresponding author:

Jake Casson, Centre for Cell Engineering, Institute of Molecular, Cell and Systems Biology (IMCSB), The University of Glasgow, Joseph Black Building, University Avenue, Glasgow G12 8QQ, UK.

Email: [j.casson.1@research.gla.ac.uk](mailto:j.casson.1@research.gla.ac.uk)



cell types communicate during the onset of dormancy may allow a deeper understanding of the cellular events involved.<sup>4</sup>

The relationship between marrow MSCs and invading BCCs has to date focussed on more traditional cell-to-cell communication routes, such as paracrine signalling via soluble proteins including cytokines.<sup>13–15</sup> More recently, attention has shifted towards extracellular vesicles (EVs) as key mediators in cell–cell communication. EVs are small extracellular membrane-enclosed vesicles that contain a variety of molecules including proteins and RNAs.<sup>16–20</sup> Increasing evidence suggests that interactions between MSCs and tumour cells involve the exchange of information via EVs.<sup>20</sup> For example, MSC-derived EVs have been reported to contain microRNAs such as miR23b,<sup>21</sup> miR21 and miR34a,<sup>22</sup> which have been found to have a tumour-suppressive effect. These EVs also contained tumour-supportive molecules, such as tissue inhibitor of metalloproteases (TIMP)-1 and -2. Within this study, we have shown that MSC-derived EVs have a negative influence on the migration and proliferation of the BCC line MCF7, with an increased adhesion. This suggests a potential role for MSC-EVs in the promotion of BCC MET and perhaps subsequent dormancy.

## Materials and methods

### Expansion cell culture

MCF7 (ATCC) cells were cultured using modified DMEM comprising 400 mL Dulbecco's modified Eagle's medium, 100 mL of medium 199, 50 mL of foetal bovine solution, 10 mL penicillin–streptomycin and 5 mL of sodium pyruvate. MCF7 cells were maintained in T75 tissue culture flasks and passaged at approximately 90% confluence using a HEPES saline wash (ThermoFisher) followed by a 3% trypsin/versine solution (ThermoFisher) to remove cells from culture flask. These cells were then centrifuged at 1400 r/min for 4 min and reseeded into new flasks, with media exchanged every 3 days. For EV isolation during MSC culture, foetal bovine serum was centrifuged for 18 h at 120,000g and supernatant was retained to exclude any EVs present.

### EV isolation

MSCs (Promocell) were grown in culture for 1 week using T150 flasks (Corning) to allow the collection of a large volume of culture medium. EVs were then isolated using the ultracentrifugation method used previously<sup>16,17</sup> and analysed via dynamic light scattering. Concentration was determined via BCA (ThermoFisher) and FluoroCet (System Biosciences) assays; generating a protein standard then adjusting isolates to the same total protein and measuring fluorescence of acetylcholinesterase (AChE), a known exosomal protein, present within the vesicles. Due

to limited supply and assessment of other EV-related studies,<sup>23–25</sup> the concentration of approximately  $2 \times 10^7$ /mL was used in each experiment.

### Transmission electron microscopy

MSC-derived (Lonza) particles were placed onto Carbon and Formvar coated copper grids from Agar Scientific. Samples were negatively stained with 2% uranyl acetate and imaged with a JEOL 1200 Transmission Electron Microscope with beam voltage of 80 kV and magnification of 200,000 $\times$ . Images generated were analysed using ImageJ to measure particle area and maximum diameter. In brief, ImageJ was used to trace the outline of the lipid membrane visible on micrographs. Software then calculated the area and maximum diameter by pixel analysis which was then converted to size using the appropriate scaling parameters.

### Generation of three-dimensional MCF7 spheroid cultures

Spheroids were generated using a similar methodology as described in Lewis et al.<sup>25</sup> Cells were initially seeded at a density of  $1 \times 10^4$  into a 24-well plate and incubated for 24 h (37°C and 5% CO<sub>2</sub>). After this initial incubation, each well of cells was cultured in a 1 mL suspension of 200 nm diameter, red fluorescently labelled magnetic iron nanoparticles (chemicell – fluidMAG-PEA) in a DMEM solution at a concentration of 0.1 mg nanoparticles/mL of media for 30 min at (37°C and 5% CO<sub>2</sub>) on top of a 24-well magnetic array plate (350 mT magnetic fields). Subsequently, the nanoparticle/DMEM suspension was removed and excess iron washed from each well using HEPES saline. Cells were then detached from the surface using trypsin and resuspended in fresh media in two opposing corners of a six-well plate to prevent disruption of individual magnetic fields. Once in solution, a 13 mm diameter magnet (producing a 350 mT magnetic field) was placed on the top of each well containing cells and incubated for 24 h while the magnetic field draws nanoparticle containing cells together to form a multicellular spheroid. Once formed, the spheroids were carefully transferred into to a liquid type I collagen gel solution, before being allowed to gel, and cultured in 1 mL fresh media.

### Collagen gel preparation

The type I collagen gel for maintaining and culturing spheroids was made up by initially premixing 0.5 mL of foetal bovine solution, 0.5 mL of modified DMEM culture media and 0.5 mL alpha-MEM. Then, 2.5 mL of rat tail collagen (2 mg/mL; First Link UK) was mixed with 1 mL of 0.1 M NaOH, before combining all together. Additional NaOH

was then titrated dropwise until entire solution turned from yellow/orange to a stable pink indicating a pH change; 1 mL of this gel solution is used to culture spheroids within a 24-well plate. A setting period of  $\leq 1$  h is permitted prior to the addition of fresh culture media.

### *Two-dimensional MCF7 migration*

The kit provided by Ibidi allowed the measurement of cell directional movement in response to a chemoattractant. Using the set protocol supplied (in the '3D Chemotaxis Assay Using  $\mu$ -Slide Chemotaxis – 2.2 2D Chemotaxis experiments without Gel'), MCF7s were seeded at a density of  $1 \times 10^6$ . Once both reservoirs were filled with 65  $\mu$ L chemoattractant-free DMEM, culture medium containing MSC-derived EVs was aspirated into the left reservoir to begin the chemoattraction for the assay. The plate was imaged using a four times objective lens at 120 s intervals over 24 h in a 37°C hot room. Results were then analysed using the ImageJ plugin 'manual tracking' and Ibidi's own 'Chemotaxis and Migration tool'.

### *Three-dimensional MCF7 migration*

To better understand MCF7 migratory processes within a bone marrow-like microenvironment, MCF7 (ATCC) spheroids were generated using magnetic nanoparticles and embedded in collagen gels before being treated over 5 days with MSC EV-doped culture medium. Images were captured using Zeiss Axio Vert A1 fluorescent microscope. Diameters were measured using ImageJ.

### *Immunocytochemistry*

Cells were fixed for 15 min in 4% formaldehyde/PBS solution. Followed by permeabilisation for 5 min at 4°C, blocking for 1 h at 37°C with 1% BSA/PBS solution. Primary antibodies (Ki67 or ALDH1A1; abcam, anti-rabbit) were diluted 1/100 with blocking solution and cells were stained overnight at room temperature before washing with 0.1% tween solution five times for 5 min. Secondary antibody was diluted 1/100 with blocking solution with the addition of 1/500 CellTag solution and incubated for 1 h at room temperature. Cells were then visualised on Licor Odyssey SA plate reader and antibody fluorescence normalised to CellTag (Supplementary Figure 1).

### *Live/dead assay*

100  $\mu$ L culture medium containing 4  $\mu$ M ethidium and 2  $\mu$ M calcein AM (Life Technologies) was added to cells and incubated at 37°C for 30 min. Cells were then washed with 1% PBS before being imaged using Zeiss Axio Vert fluorescence microscope at 20 $\times$  magnification where cells containing calcein or ethidium were counted.

### *Adhesion assay*

Monolayers were seeded in a 96-well plate and allowed to attach. A dilution series of MSC-derived EVs was then applied to these for 24 h. Following this period, cells trypsinised and reseeded into a new 96-well plate. These cells were allowed to attach for 30 min before the culture medium was removed. Remaining cells were stained with DAPI for 15 min before being visualised at 20 $\times$  magnification. The presence of nuclei in 10 random fields was counted across three wells for each MSC EV concentration.

## **Results and discussion**

### *Quantification of MSC-derived EVs isolated from conditioned culture medium*

EVs isolated from MSC culture medium were quantified using dynamic light scattering and Fluorocet assay. Dynamic light scattering allows the size of particles to be determined (Figure 1(a)) indicating highest peak intensities at 91.3 and 164 nm, with a weighted average diameter of 174.4 nm (Figure 1(b)). This indicates the presence of two vesicle populations: exosomes and larger microvesicles. AChE fluorescence was then assayed (Figure 1(c)) following protein quantification to determine the number of MSC-derived EVs present, found to be  $1.6 \times 10^9$ /mL. The presence of MSC-derived EVs using this method of isolation is indicated by TEM (Figure 1(b)).

### *MCF7 cells migrate away from MSC EVs*

The effect of MSC-derived EVs on MCF7 cell motility was assessed. Within standard two-dimensional culture, MCF7 cells grown in control culture medium did not migrate preferentially in any direction (Figure 2(b)); however, when treated with cell culture medium containing purified MSC-derived EVs, they become more mobile (Figure 2(a)). Interestingly, they do not move towards the MSC-derived EVs, but appear to migrate away from them. This phenomenon is quite pronounced over 24 h, with no MCF7 cells migrating towards the MSC-derived EVs. This observation therefore appears to support MCF7 cells in monolayer (Figure 2), where the cells are compacting within the spheroids as opposed to migrating out towards the EV stimulus. Over 120 h, mean spheroid area decreases in the presence of MSC-derived EVs (Figure 3(e)).

Consequently, 3D MCF7 cell spheroids were then cultured within a bone marrow-like environment (type I collagen gel) and challenged with MSC-derived EVs. Through measuring the spheroid diameter, it was noted that the spheroids become more compacted over time in response to the EVs when compared to control culture conditions, where instead spheroids increased in diameter by approximately 10% over a 24-h period (Figure 3(a)–(e)). Using a

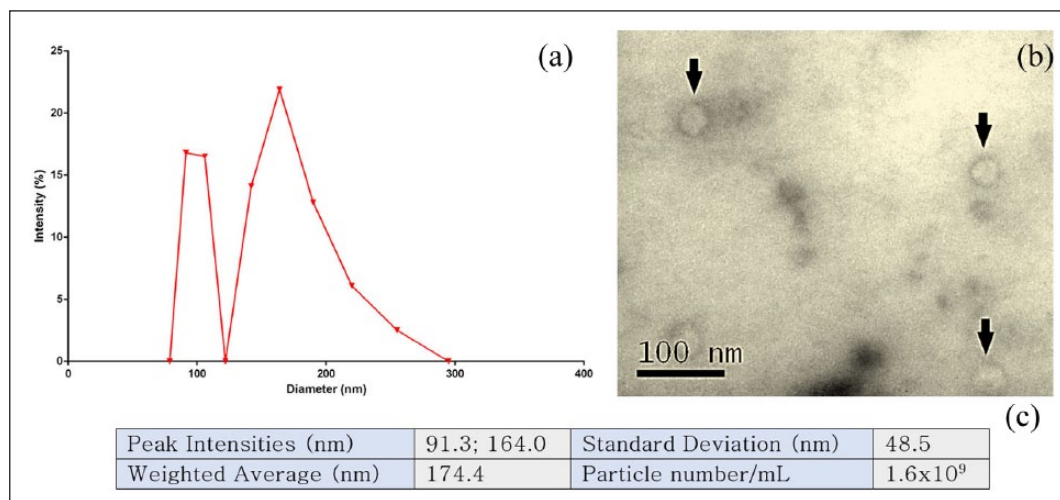


**Figure 1.** MSC-derived EVs (a) measured using dynamic light scattering and average intensities plotted ( $n=3$ ). (b) Transmission electron microscope image of MSC-derived EVs; arrows indicate the presence of vesicles (c) A table detailing key data from dynamic light scatter in addition to particle number acquired through measurement of AChE fluorescence using Fluorocet assay.

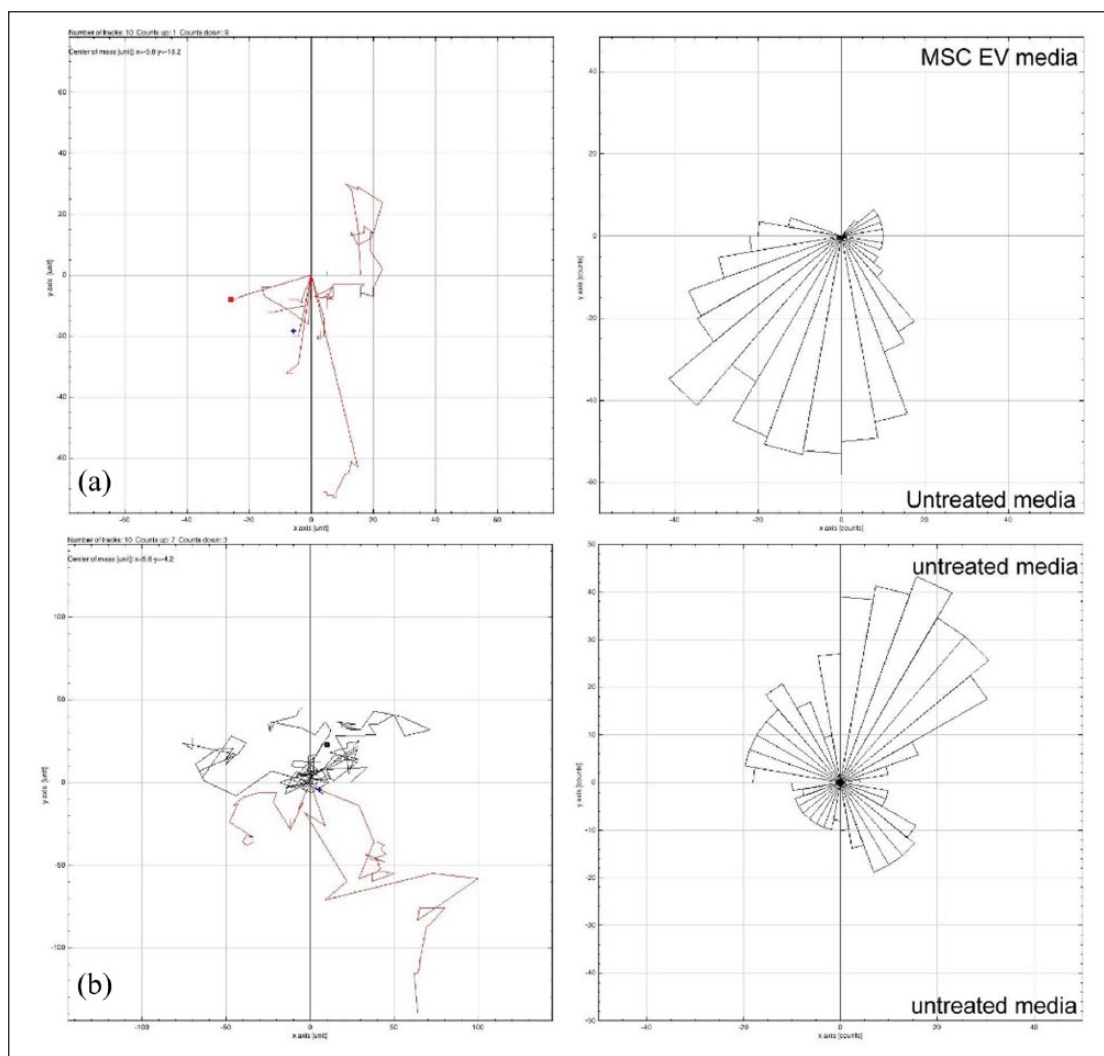


**Figure 2.** MCF7 cells cultured over 24h with (a) culture medium containing MSC-derived EVs or (b) control medium, without EVs (10 cells tracked in each condition using ImageJ).

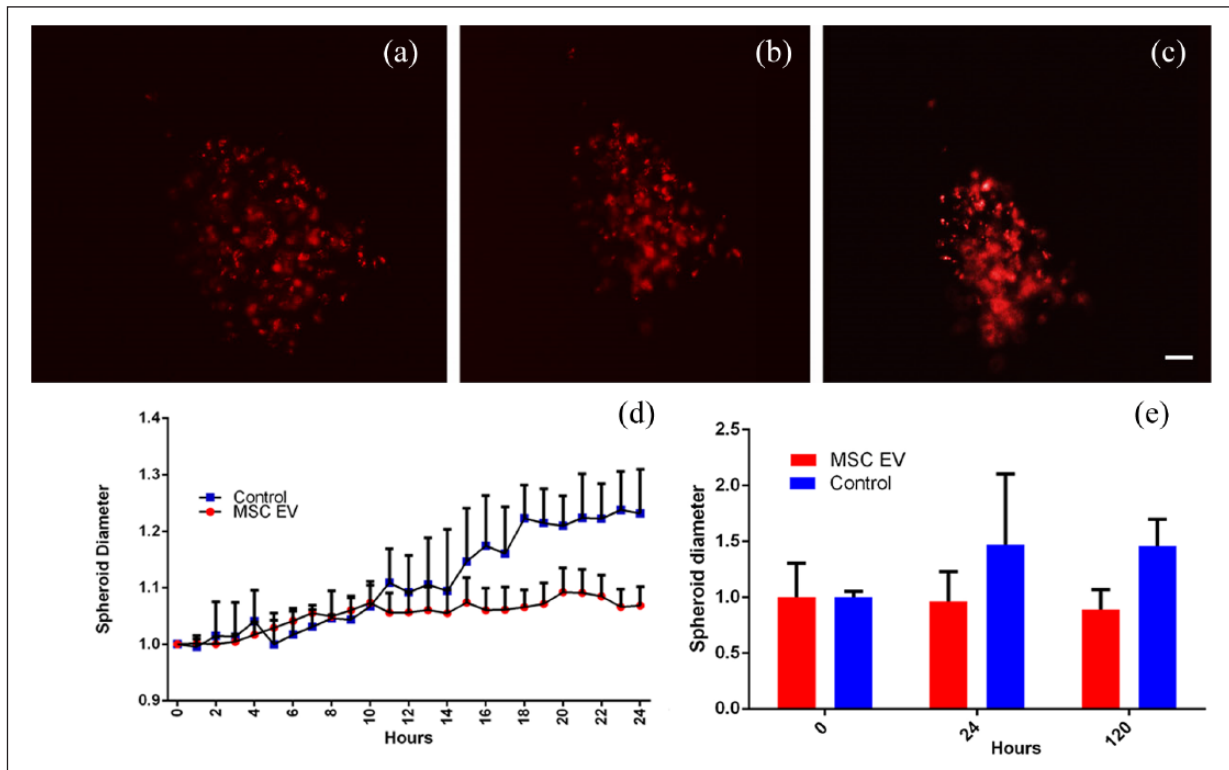


**Figure 3.** MCF7 spheroid cultured with MSC-derived EVs for (a) 0h, (b) 24h and (c) 120h; note the apparent decrease in diameter; (d) 24-h time lapse of spheroid treated with MSC-derived EVs spheroid diameter normalised to 0h,  $n=3$ ; (e) measurements of further MCF7 spheroids at hours 0, 24 and 120 normalised to 0-h average ( $n \geq 4$ ; scale bar = 10  $\mu\text{m}$ ; images recorded using Zeiss Axio Vert A1 microscope).

two-way analysis of variance (ANOVA) the difference in spheroid size is significant ( $p=0.0011$ ).

### *MSC EVs cause decreased proliferation and increase adhesion of MCF7 cells*

It has previously been described that MSCs possess the capacity for tumour growth and suppression.<sup>26,27</sup> Therefore, to further study the effect of MSC-derived EVs upon MCF7 cells, cell proliferation, stem cell-like phenotype and cell adhesion were assessed. ALDH1A1 is a protein that is present in malignant BCCs which have undergone EMT<sup>28</sup> and as such is an established cancer stem cell marker;<sup>29,30</sup> a lower ALDH1A1 expression correlates with a less active, stem cell-like cell. Here, following exposure to purified MSC-derived EVs, MCF7 cells demonstrated a decrease in ALDH1A1 (Figure 4(a)), indicating that the cells are exhibiting a less active/tumourigenic cell phenotype.<sup>31,32</sup> Indeed, ALDH1A1 levels decreased with increased EV concentration, suggesting an inverse correlation.

Confirmation of this lower tumourigenicity was achieved via quantification of Ki67 protein levels. Ki67 is a protein that is present in all stages of cell cycle except  $G_0$  and is strongly associated with tumour cell proliferation

and growth; clinically, it has been shown to correlate with metastasis and the clinical stage of tumours.<sup>33,34</sup> In this study, exposure to MSC-derived EVs caused a significant decrease ( $p < 0.005$ ) in Ki67 expression in MCF7 cells (Figure 4(b)); again, an inverse correlation was noted. This suggests that MCF7 cells have reduced proliferation and may have initiated a switch to a dormant state in response to the MSC EVs. MCF7 cells cultured with MSC EVs in monolayer were assayed for viability over 5 days. No significant change in cell viability was seen (supplementary Figure 2).

An increased cell adhesion is key to an epithelial cell phenotype. Therefore, in addition to probing for intracellular protein markers, MCF7 monolayers were cultured with MSC-derived EVs for 24h and subsequent cell adhesion potential was assessed. A reciprocal relationship was observed, with a significant increase in MCF7 adhesion alongside increasing MSC-derived EV concentration (Figure 4(c)). Collectively, this correlates with a decrease in ALDH1A1 and proliferation, with the MSC-derived EVs reinforcing an epithelial cell phenotype. Expression of EMT marker genes was analysed in MCF7 spheroids cultured in the presence or absence of MSC spheroids to establish the effect of MSC paracrine signalling, including EVs, on MCF7 EMT. Results indicated that MCF7

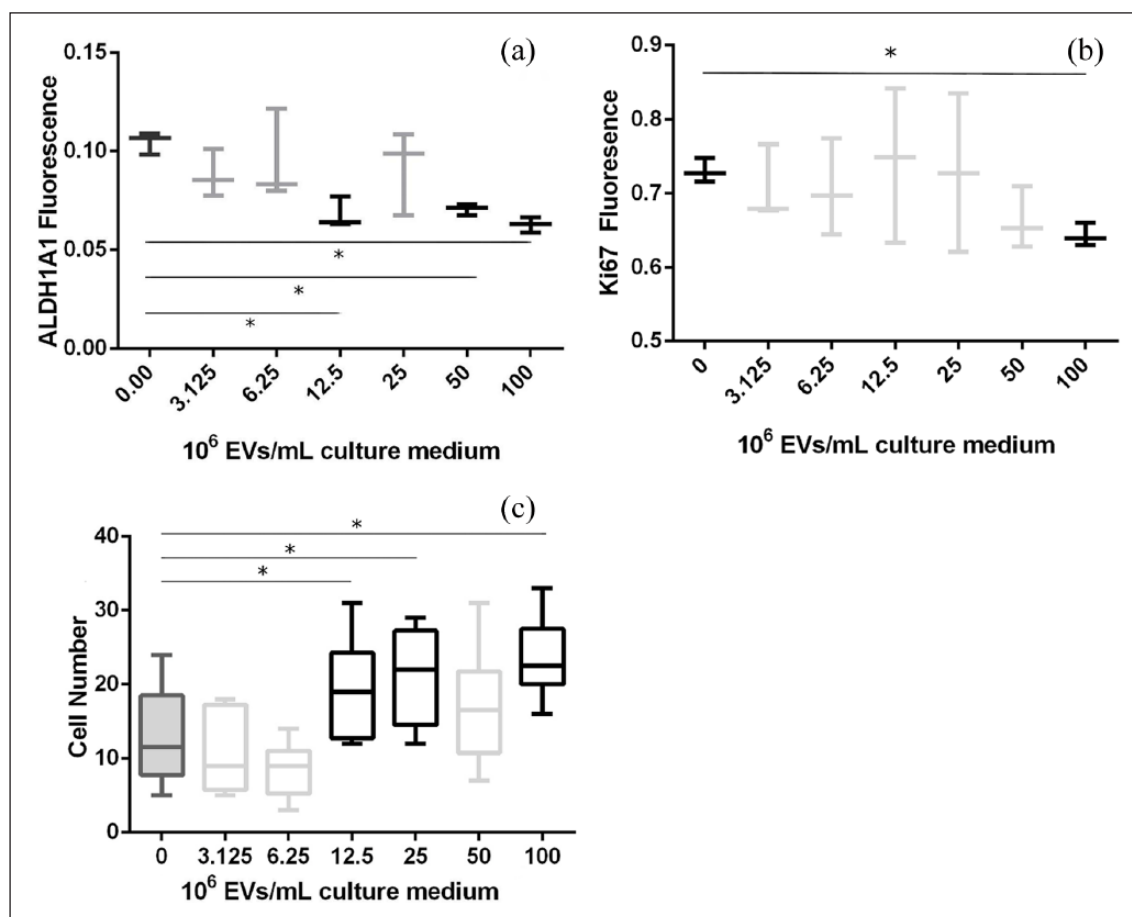


**Figure 4.** MCF7 cells treated with a dilution series of purified MSC-derived EVs for 24 h before being probed for (a) the cancer stem cell marker, ALDH1A1, and (b) the proliferation marker, Ki67 (relative fluorescence calculated via normalisation to CellTag 700;  $n = 3$ ). (c) MCF7 adhesion assay following pre-treatment with MSC-derived EVs for 24 h (10 fields from 3 wells;  $20\times$  magnification). Asterisks denote  $p < 0.005$  versus control condition.

spheroids co-cultured with MSC spheroids had an increase in the EMT markers e-cadherin and keratin19, with a reduction in mesenchymal markers vimentin and JUP. This suggests that MSCs encouraged a transition to the epithelial state (Supplementary Figure 3).

## Conclusion

BCC metastasis into the bone marrow niche involves a complex series of paracrine signalling and cell-cell interactions. However, here we show that treating MCF7 cells with just MSC-derived EVs appears to initiate an epithelial cell phenotype with potential dormancy. This suggests that MSC-derived EVs contribute to the net loss in tumourigenicity of invading BCCs, allowing them to engraft within the marrow in a cycling quiescent state, ultimately resulting in anti-cancer drug resistance. The two peaks seen in Figure 1 indicate a mixed population of both exosomes and larger microvesicles; these are trafficked out of the cell in different ways and as such their contents may also be different. While there is some evidence in support of the role of microRNAs in

initiating dormancy,<sup>4,21</sup> further research into the cargo of both populations of EVs is necessary, namely which proteins and small molecules/metabolites may be involved in BCC dormancy.

## Acknowledgements

C.C.B. conceived and designed the experiments, and assisted in writing the paper; J.C. and O.G.D. performed the experiments; J.C. analysed the data; J.C. wrote the paper; C.-A.S. assisted in the experiments; O.G.D. provided EV isolation technique and expertise and M.J.D. provided MSCs and expertise in experimental design.

## Declaration of conflicting interests

The author(s) declared no potential conflicts of interest with respect to the research, authorship, and/or publication of this article.

## Funding

The author(s) disclosed receipt of the following financial support for the research, authorship and/or publication of this article: The

authors would like to reference funding from the BBSRC for this work, grant reference number BB/L008661/1.

## ORCID iD

Jake Casson  <https://orcid.org/0000-0003-0719-1295>

## Supplemental Material

Supplemental material is available for this article online.

## References

1. Cancer Research UK. Breast cancer statistics, 2016, <https://www.cancerresearchuk.org/health-professional/cancer-statistics/statistics-by-cancer-type/breast-cancer#heading-zero> (accessed 2 July 2018).
2. Hüsemann Y, Geigl JB, Schubert F, et al. Systemic spread is an early step in breast cancer. *Cancer Cell* 2008; 13(1): 58–68.
3. American Cancer Society. Bone metastasis key statistics, 2014, <http://www.cancer.org/treatment/understandingyour-diagnosis/bonemetastasis/bone-metastasis-key-statistics1> (accessed 7 April 2018).
4. Bliss SA, Sinha G, Sandiford O, et al. Mesenchymal stem cell-derived exosomes stimulates cycling quiescence and early breast cancer dormancy in bone marrow. *Cancer Res* 2016; 76: 1092.
5. Diel IJ, Kaufmann M, Goerner R, et al. Detection of tumor cells in bone marrow of patients with primary breast cancer: a prognostic factor for distant metastasis. *J Clin Oncol* 1992; 10(10): 1534–1539.
6. Liu F, Gu LN, Shan BE, et al. Biomarkers for EMT and MET in breast cancer: an update. *Oncol Lett* 2016; 12(6): 4869–4876.
7. Yeung KT and Yang J. Epithelial-mesenchymal transition in tumor metastasis. *Mol Oncol* 2017; 11(1): 28–39.
8. Tsai JH and Yang J. Epithelial-mesenchymal plasticity in carcinoma metastasis. *Gene Dev* 2013; 27(20): 2192–2206.
9. Walker ND, Patel J, Munoz JL, et al. The bone marrow niche in support of breast cancer dormancy. *Cancer Lett* 2016; 380(1): 263–271.
10. Psaila B and Lyden D. The metastatic niche: adapting the foreign soil. *Nat Rev Cancer* 2009; 9(4): 285.
11. Khoon MCS. Experimental models of bone metastasis: opportunities for the study of cancer dormancy. *Adv Drug Deliver Rev* 2015; 94: 141–150.
12. Zhang XHF, Giuliano M, Trivedi MV, et al. Metastasis dormancy in estrogen receptor-positive breast cancer. *Clin Cancer Res* 2013; 19(23): 6389–6397.
13. Luker KE and Luker GD. Functions of CXCL12 and CXCR4 in breast cancer. *Cancer Lett* 2016; 238(1): 30–41.
14. Liu S, Ginestier C, Ou SJ, et al. Breast cancer stem cells are regulated by mesenchymal stem cells through cytokine networks. *Cancer Res* 2011; 71(2): 614–624.
15. Casson J, O’Kane S, Smith CA, et al. Interleukin 6 plays a role in the migration of magnetically levitated mesenchymal stem cells spheroids. *Appl Sci* 2018; 8(3): 412.
16. Davies OG, Cox SC, Williams RL, et al. Annexin-enriched osteoblast-derived vesicles act as an extracellular site of mineral nucleation within developing stem cell cultures. *Sci Rep* 2017; 7(1): 12639.
17. Robbins PD and Morelli AE. Regulation of immune responses by extracellular vesicles. *Nat Rev Immunol* 2014; 14(3): 195.
18. Yáñez-Mó M, Siljander PRM, Andreu Z, et al. Biological properties of extracellular vesicles and their physiological functions. *J Extracell Vesicles* 2015; 4(1): 27066.
19. Wu J, Qu Z, Fei ZW, et al. Role of stem cell-derived exosomes in cancer. *Oncol Lett* 2017; 13(5): 2855–2866.
20. Ono M, Kosaka N, Tominaga N, et al. Exosomes from bone marrow mesenchymal stem cells contain a microRNA that promotes dormancy in metastatic breast cancer cells. *Sci Signal* 2014; 7(332): ra63.
21. Vallabhaneni KC, Penformis P, Dhule S, et al. Extracellular vesicles from bone marrow mesenchymal stem/stromal cells transport tumor regulatory microRNA, proteins, and metabolites. *Oncotarget* 2015; 6(7): 4953.
22. Del Fattore A, Luciano R, Saracino R, et al. Differential effects of extracellular vesicles secreted by mesenchymal stem cells from different sources on glioblastoma cells. *Expert Opin Biol Ther* 2015; 15(4): 495–504.
23. Salomon C, Ryan J, Sobrevia L, et al. Exosomal signaling during hypoxia mediates microvascular endothelial cell migration and vasculogenesis. *PLoS ONE* 2013; 8(7): e68451.
24. Gong L, Bao Q, Hu C, et al. Exosomal miR-675 from metastatic osteosarcoma promotes cell migration and invasion by targeting CALN1. *Biochem Biophys Res Commun* 2018; 500(2): 170–176.
25. Lewis EEL, Wheadon H, Lewis N, et al. A quiescent, regeneration-responsive tissue engineered mesenchymal stem cell bone marrow niche model via magnetic levitation. *ACS Nano* 2016; 10(9): 8346–8354.
26. Lee JK, Park SR, Jung BK, et al. Exosomes derived from mesenchymal stem cells suppress angiogenesis by down-regulating VEGF expression in breast cancer cells. *PLoS ONE* 2013; 8(12): e84256.
27. Li W, Ma H, Zhang J, et al. Unraveling the roles of CD44/CD24 and ALDH1 as cancer stem cell markers in tumorigenesis and metastasis. *Sci Rep* 2017; 7(1): 13856.
28. Vazquez-Santillan K, Melendez-Zajgla J, Jimenez-Hernandez LE, et al. NF-kappaB-inducing kinase regulates stem cell phenotype in breast cancer. *Sci Rep* 2016; 6: 37340.
29. Marcatto P, Dean CA, Pan D, et al. Aldehyde dehydrogenase activity of breast cancer stem cells is primarily due to isoform ALDH1A3 and its expression is predictive of metastasis. *Stem Cells* 2011; 29(1): 32–45.
30. Ma F, Li H, Li Y, et al. Aldehyde dehydrogenase 1 (ALDH1) expression is an independent prognostic factor in triple negative breast cancer (TNBC). *Medicine* 2017; 96(14): e6561.
31. Tomita H, Tanaka K, Tanaka T, et al. Aldehyde dehydrogenase 1A1 in stem cells and cancer. *Oncotarget* 2016; 7(10): 11018.
32. Li LT, Jiang G, Chen Q, et al. Ki67 is a promising molecular target in the diagnosis of cancer. *Mol Med Rep* 2015; 11(3): 1566–1572.
33. Scholzen T and Gerdes J. The Ki-67 protein: from the known and the unknown. *J Cell Physiol* 2000; 182(3): 311–322.
34. Lin R, Wang S and Zhao RC. Exosomes from human adipose-derived mesenchymal stem cells promote migration through Wnt signaling pathway in a breast cancer cell model. *Mol Cell Biochem* 2013; 383(1–2): 13–20.